

Flutter and buffeting responses of the Shantou Bay Bridge

M. Gu[†], W. Chen[‡], L. D. Zhu^{††}, J. Z. Song^{††} and H. F. Xiang^{†††}

State Key Laboratory for Disaster Reduction in Civil Engineering, Tongji University, 200092 Shanghai, China

Abstract. Shantou Bay Bridge is the first long-span suspension bridge in China. Because of its location near the Shantou Seaport and its exposure to high typhoon winds, wind-resistant studies are necessary to be made. In this paper, critical flutter wind speeds and buffeting responses of this bridge at its operation and main construction stages are investigated. The Buffeting Response Spectrum method is first briefly presented. Then the sectional model test is carried out to directly obtain the critical flutter wind speed and to identify the flutter derivatives, which are adopted for the later analysis of the buffeting responses using the Buffeting Response Spectrum method. Finally the aeroelastic full bridge model is tested to further investigate the dynamic effects of the bridge. The results from the tests and the computations indicate that the flutter and buffeting behaviors of the Shantou Bay Bridge are satisfied.

Key words: suspension bridge; sectional model; aeroelastic full bridge model, flutter; buffeting.

1. Introduction

It has been recognized that wind responses of long-span bridges mainly include buffeting response due to wind turbulence and self-excited vibrations, such as flutter, vortex shedding and galloping. Among these wind-induced vibrations flutter and buffeting responses are the most concerned problems. A spring-suspended sectional deck model, which simulates the frequencies, distributions of the mass and inertial moment of mass as well as damping, can be used to directly estimate the critical flutter wind speed for most cases. The model can also be tested to identify the flutter derivatives from the vibration signals for flutter and buffeting analyses. The method originally developed by Scanlan and Tomko in (1971) has been improved by researchers (Jain *et al.* 1996, Chen *et al.* 1999, Giana *et al.* 1999) for estimating critical flutter wind speed of bridges. The other analysis method proposed also by Scanlan (1977) is the base of present studies on buffeting responses of bridges. The buffeting forces are constructed based on quasi-steady theory, and the aeroelastic effect due to wind-structure coupling is described by the flutter forces as in flutter analysis method (Scanlan and Tomko 1971). In Scanlan's original method, aerodynamic admittance functions are taken to be unity, which may lead to an overestimation of the buffeting response. Liepmann's simplified expression of Sears function was adopted as the aerodynamic admittance

[†] Professor

[‡] Associate professor

^{††} Associate professor

^{†††} Professor

^{††††} Professor

functions for the analysis of the buffeting responses of the Nanpu Bridge with a main span of 423 m (Gu and Xiang 1991), and other bridges in China. For practical purpose, Buffeting Response Spectrum method was developed in (Chen *et al.* 1995) based on the Scanlan's method and on detailed parametric analyses. This method has been proven to be not only convenient but also precise enough for practical purpose through analyses of buffeting responses of several long-span cable-stayed bridges in China, and recently has been adopted into *Chinese Guideline for Wind-resistance Design of Highway Bridges* (Xiang *et al.* 1996).

In recent years, more than 40 long-span cable-stayed bridges and several suspension bridges have been built or are being constructed in China. The wind-resistant studies on these bridges have been carried out by the authors and other researchers. The Shantou Bay Bridge with a main span of 452 meters is the first long-span suspension bridge in China. Although the span of this bridge is not very long, wind-resistance study is necessary to be made on this bridge in view of its location near the Shantou Seaport and the exposure to high typhoon winds.

In this paper, Buffeting Response Spectrum method is first briefly presented. The critical flutter wind speeds of the Shantou Bay Bridge at some selected critical erection stages and operation stage are then obtained through wind tunnel tests on the spring-suspended sectional model of the bridge. After that, the buffeting responses of this bridge are analyzed using Buffeting Response Spectrum method, and finally the full bridge aeroelastic model is tested to further investigate the flutter and buffeting characteristics of this bridge.

2. Buffeting Response Spectrum method

Buffeting Response Spectrum method (Chen *et al.* 1995) was adopted in the analysis of the buffeting responses of the Shantou Bay Bridge. Thus this method is firstly briefly introduced. The motion equation of i th generalized coordinate of the bridge under the action of natural wind is expressed as

$$I_i(\ddot{\xi}_i + 2\zeta_i\omega_i\dot{\xi}_i + \omega_i^2\xi_i) = q_i(t) \quad (1)$$

where ξ_i is the i th generalized coordinate; I_i is the i th generalized mass or inertial moment of mass; ω_i is the i th circular frequency; ζ_i is the i th damping ratio; $q_i(t)$ is the i th generalized force, which has the form as

$$q_i(t) = \int_0^L \{ [L_{ae}(x, t) + L_b(x, t)]h_i(x)B + [D_{ae}(x, t) + D_b(x, t)]p_i(x)B + [M_{ae}(x, t) + M_b(x, t)]\alpha_i(x) \} dx \quad (2)$$

in which, $L_{ae}(x, t)$, $D_{ae}(x, t)$ and $M_{ae}(x, t)$ are the aeroelastic lift, drag and pitching moment, respectively; $L_b(x, t)$, $D_b(x, t)$ and $M_b(x, t)$ are the buffeting lift, drag and pitching moment, respectively. The aeroelastic forces are the same as those defined in (Scanlan 1977). The buffeting forces also take the Scanlan's expressions (Scanlan 1977, Simiu and Scanlan 1978) with consideration of aerodynamic admittance functions in them. The aerodynamic admittance function in frequency domain is simply expressed in the present analysis with Liepmann expression of Sears function (Liepmann 1952) :

$$|\chi(\omega)|^2 = \frac{1}{1 + \pi\omega B/U} \quad (3)$$

Using random vibration theory and based on detailed parametric analyses, the Buffeting Response Spectrum method can be developed and the RMS buffeting displacements and torsional angle can be easily found using the following equations

$$\sigma_{hi} = C_{oh}C_G C_{Bh}C_{Ah}C_{zhi}\varphi(\beta_h)\mu(\tilde{K}_{hi})\phi_{wh}(f_{hi}) \quad (4)$$

$$\sigma_{pi} = C_{op}C_G C_{Bp}C_{Ap}C_{zpi}\varphi(\beta_p)\mu(\tilde{K}_{pi})\phi_{wp}(f_{pi}) \quad (5)$$

$$\sigma_{\alpha i} = C_{o\alpha}C_G C_{B\alpha}C_{A\alpha}C_{z\alpha i}\varphi(\beta_\alpha)\mu(\tilde{K}_{\alpha i})\phi_{w\alpha}(f_{\alpha i}) \quad (6)$$

where σ_{hi} , σ_{pi} and $\sigma_{\alpha i}$ are the RMS buffeting values of vertical bending displacement, lateral bending displacement and torsional angle, respectively; $C_{oh} = 0.866\rho$, $C_{op} = 0.001\rho$, $C_{o\alpha} = 0.433\rho$; $C_G = 0.4/\ln(z/z_0)$; $C_{Bh} = C_{Bp} = B^2\sqrt{z\bar{B}}/m$, $C_{B\alpha} = B^4\sqrt{z\bar{B}}/I$; $C_{Ah} = C_L' + (A/B)C_D$, $C_{Ap} = (A/B)C_D$, $C_{A\alpha} = C_M'$; $\tilde{K}_{hi} = K_{hi}$, $\tilde{K}_{pi} = K_{pi}$, $\tilde{K}_{\alpha i} = K_{\alpha i}\sqrt{1 - \rho B^4 A_3^*/I}$, C_{zh} , $C_{z\alpha}$ and C_{zp} are mainly relative to the structural damping and aerodynamic damping, and they have the following forms,

$$C_{zhi} = \frac{1}{\sqrt{\zeta_{hi} - \rho B^2 H_1^*/2m}}, \quad C_{zpi} = \frac{1}{\sqrt{\zeta_{zpi} - \rho B^2 P_1^*/2m}}, \quad C_{z\alpha i} = \frac{1}{\sqrt{\zeta_{\alpha i} - \rho B^2 A_2^*/2I}} \quad (7)$$

$\varphi(\beta)$, which reflects the joint acceptance function with sine function replacing the mode shape, is written as

$$\varphi(\beta) = \frac{1}{p^2 + \beta^2} \left(\beta + \frac{2p^2}{p^2 + \beta^2} \right) \quad (8)$$

in which $p = \pi$ for the first symmetric mode or $p = 2\pi$ for the first asymmetric mode shape; $\beta = \lambda LK / (2\pi B)$; $\mu(K)$ is a function of the aerodynamic admittance functions: $\mu(K) = 1/\sqrt{K^3(1 + \pi K)}$ for Liepmann's expression of Sears function, while $\mu(K) = 1/\sqrt{K^3}$ for unity aerodynamic admittance; $\phi_{wh}(f)$, $\phi_{wp}(f)$ and $\phi_{w\alpha}(f)$ indicate the influence of wind spectra and aerodynamic force coefficients and $f = zK/(2\pi B)$. They take the following forms,

$$\phi_{wh}(f) = \frac{\delta_h(f)}{1 + 4f}, \quad \phi_{wp}(f) = \frac{1}{(1 + 50f)^{5/6}}, \quad \phi_{w\alpha}(f) = \frac{\delta_\alpha(f)}{1 + 4f} \quad (9)$$

in which δ_h and δ_α are modification factors. If $C_L' \gg C_L$, $C_M' \gg C_M$ and $C_L' \gg (A/B)C_D$, δ_h and δ_α take 1; otherwise, the following formulae can be used for modification,

$$\delta_h(f) = \left[1 + \left(\frac{2C_L}{C_L' + (A/B)C_D} \right)^2 \frac{S_{uu}(f)}{S_{ww}(f)} \right]^{1/2} \quad (10)$$

$$\delta_\alpha(f) = \left[1 + \left(\frac{2C_M}{C_M'} \right)^2 \frac{S_{uu}(f)}{S_{ww}(f)} \right]^{1/2} \quad (11)$$

All the values of the above equations have been expressed in data tables or graphic curves in the *Chinese Guideline for Wind-resistance Design of Highway Bridges* (Xiang *et al.* 1996). This method has been proved much convenient for practical use, such as for code and standard uses. Its precision is also satisfied for practical purpose (Chen *et al.* 1995, Xiang *et al.* 1996).

The estimated total buffeting response can finally be composed of the concerned mode responses using SRSS method.

3. Dynamic characteristics of the Shantou Bay Bridge

Figs. 1 and 2 show the elevation and general view of the cross-section of the deck of Shantou Bay Bridge, respectively. The deck section has a curved bottom, as shown in Fig. 2.

At the construction stage, each deck section is 5.7 meters in length and about 24 meters in width (see Fig. 2), with a gap of 30 centimeters between two sections. These sections are temporarily connected each other with connecting members, which provides the deck with larger lateral bending stiffness and torsion stiffness, compared with smaller vertical bending stiffness. In addition, during the construction of the bridge, the deck sections are erected from its pylons to the center of the mid-span and the side piers simultaneously. On this basis, the dynamic behaviors of the bridge at four critical erection stages shown in Fig. 3 were analyzed.

At the Stages A, B and C in Fig. 3, four ends of the deck sections are all free; while at the Stage D, the mid-span decks individually from the two pylons are jointed each other, and the side span

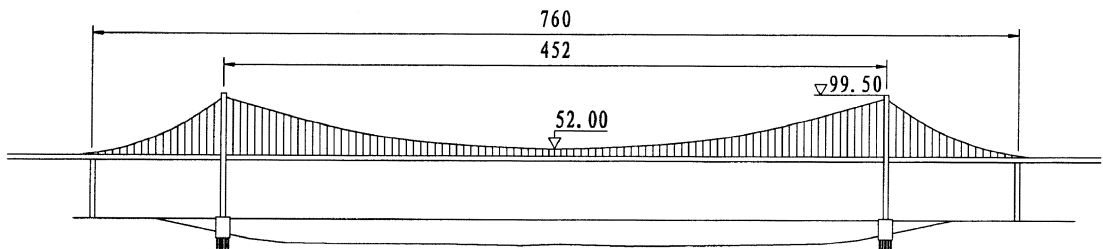


Fig. 1 General view of elevation of the bridge

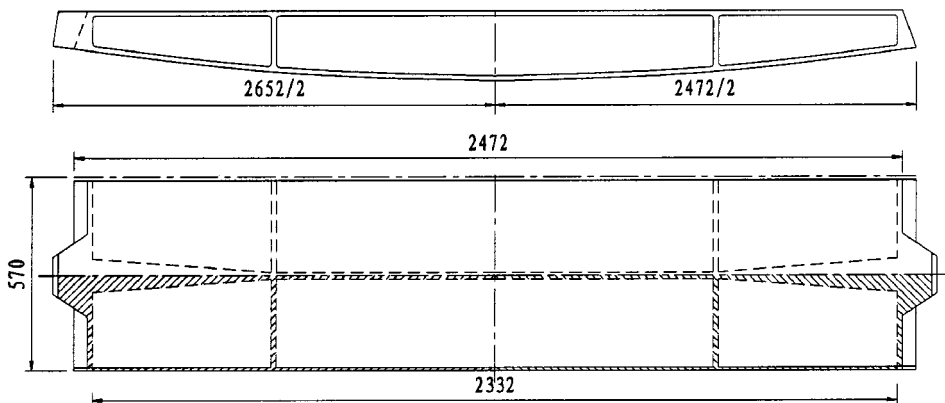


Fig. 2 General view of the deck cross section

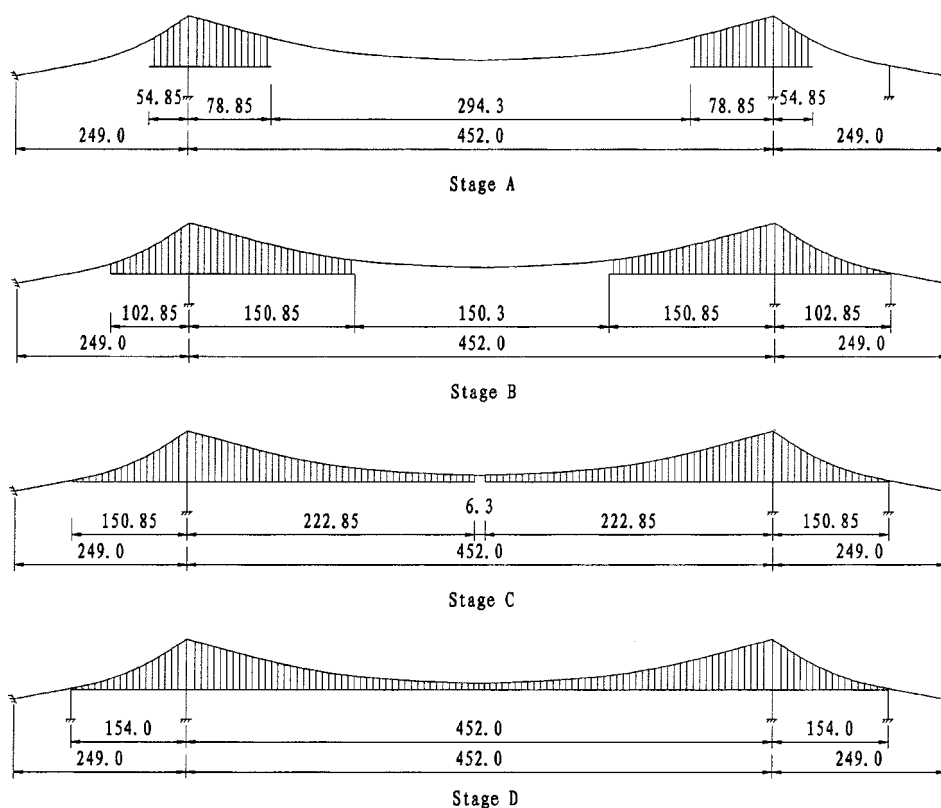


Fig. 3 Construction stages for analysis

Table 1 The main natural frequencies (H_z) of the Shantou Bay Bridge

		Vertical bending			Lateral bending		Torsional
		1st	2nd	3rd	1st	2nd	1st
Stage C	Computed	0.142	0.170	0.254	0.094	0.139	0.577
	Measured	0.154	0.180	0.265	0.10		0.571
	Error(%)	7.8	5.5	4.2	6.0		1.0
Stage D	Computed	0.170	0.174	0.255	0.201	0.521	0.612
	Measured	0.170	0.180	0.260	0.190		0.595
	Error(%)	0.0	3.3	2.0	5.5		2.8
Stage E	Computed	0.184	0.199	0.301	0.229	0.591	0.593
	Measured	0.190	0.195	0.305	0.220	0.571	0.610
	Error(%)	3.2	2.1	1.3	4.1	3.5	2.8

decks are also jointed to the side piers. In computations of the dynamic behaviors, it was taken into consideration that the tension and the location of the main cables vary with the process of the deck erection. Stage E denotes the operation stage.

The main computed results of the natural frequencies of the bridge at the four erection stages are

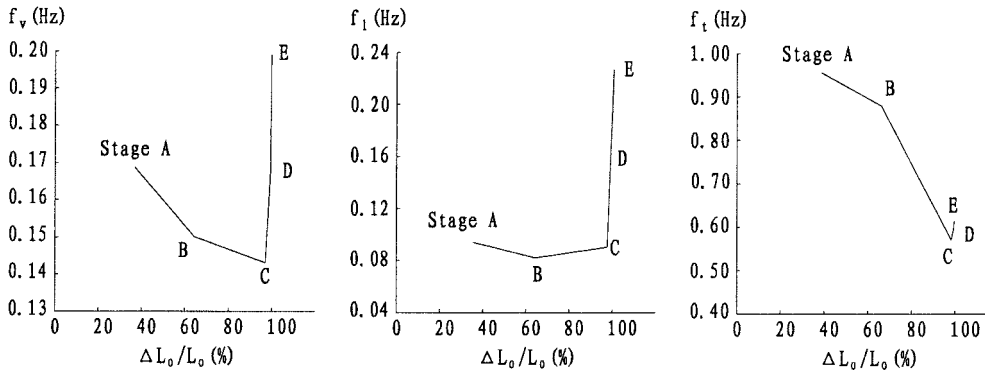


Fig. 4 The first model frequencies versus the erected length of the deck

given in Table 1, together with the measured frequencies from the full bridge aeroelastic model. Fig. 4 shows the variation of the main natural frequencies with the erection process, where L is the erected mid-span deck length; L_0 is the total mid-span deck length. It is seen that the first vertical bending frequency continuously decreases from the Stage A to Stage B and Stage C, and then increases from the Stage C to Stage D and Stage E. The first lateral frequencies at the Stages A, B and C are almost the same; and the first lateral frequency varies from the Stage C to Stage D and then to Stage E in the similar manner as the first vertical bending frequency does. The first torsional frequency is seen to decrease largely with the increase of the erected deck length. In addition, there is only a little difference among the first torsional frequencies at the Stages C, D and E.

From the results of the dynamic analysis, Stages C, D and E are critical, and the wind dynamic effects at these stages need to be further theoretically and experimentally studied.

4. Reference wind speed and design wind speed

A meteorological observatory located in the suburb of the Shantou City provided the measured wind speed records of 32 years, from 1959 to 1991. During these years, there were sixteen typhoon records higher than 8th Beaufort level. The wind speed records were then used as the statistical samples to deduce the reference wind speed at the observatory site, which is 37.4 m/s. In addition, other two temporary observatories were built on the Mayu Island, which will be connected to Shantou City with the Shantou Bay Bridge, and the Guangao District, much near the Mayu Island and facing to open-sea. The limited wind speed records from these two temporary observatories and the wind records from the meteorological observatory in the suburb of the Shantou City were used to produce a ratio of mean wind speeds at the meteorological observatory located in the suburb of the Shantou City and the bridge site. The ratio is 1.31. According to this wind speed ratio and the wind speed records from the meteorological observatory the reference wind speed, namely 10-min average and 100-year return period wind speed at 10-m height, at the bridge site could be deduced as

$$U_{10} = 49 \text{ m/s} \quad (12)$$

The design wind speed for the bridge was then given according to *Chinese Guidelines for Wind-Resistance of Highway Bridges* (Xiang *et al.* 1996) as follows,

$$U_d = U_{10}(50/10)^{1/8} = 60 \text{ m/s} \quad (13)$$

where 50 (unit in m) means that the bridge deck has a clearance of 50 meters above water. This wind speed was used to check the buffeting responses of the bridge.

The flutter design wind speed thus was (Xiang *et al.* 1996) :

$$[U_c] = 1.2\mu_f U_d = 1.2 \times 1.175 \times 60 = 85 \text{ m/s} \quad (14)$$

The wind speeds for the bridge at the erection stage were (Xiang *et al.* 1996) :

$$(U_d)_e = 0.7 \times 60 = 42 \text{ m/s}, \quad \text{for checking the buffeting response;} \quad (15)$$

$$[U_c]_e = 0.7 \times 85 = 60 \text{ m/s}, \quad \text{for checking the critical flutter wind speed.} \quad (16)$$

5. Sectional model test

The sectional model of the Shantou Bay Bridge was tested to measure the static drag, lift and torsional moment coefficients as a function of wind attack angle using a strain balance. The testing results for the operation stage are given in Fig. 5. In addition, the same model supported by springs with a structural damping ratio of about 0.02 was tested in smooth flow at -3° , 0° and $+3^\circ$ wind attack angles to obtain the critical flutter wind speeds and the flutter derivatives. The flutter derivatives were used for the later analysis of the buffeting responses. The model tests were conducted in the TJ-1 Boundary Layer Wind Tunnel in Tongji University, whose working section is 1.2 meters wide, 1.8 meters high and 18 meters long. The wind speed ranges from about 1 to 32 m/s.

To obtain the critical flutter wind speeds of the bridge at the critical construction stages and the operation stage, the section model was designed and fabricated in terms of some simulation rules, i.e.,

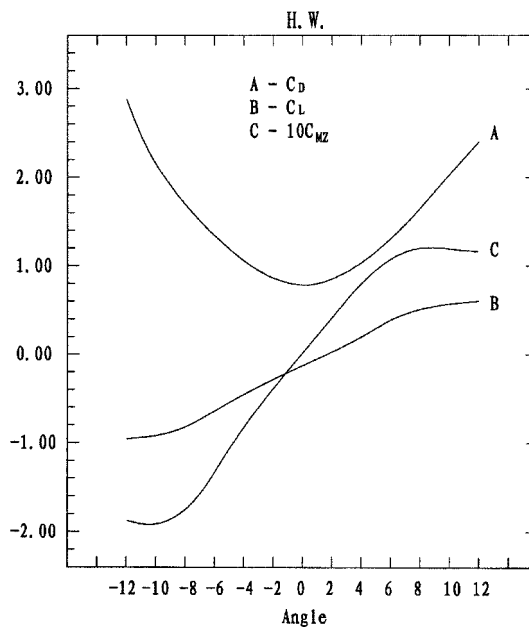


Fig. 5 Static force coefficients of the bridge deck for operation stage

$$\frac{U_m}{\omega_m B_m} = \frac{U_p}{\omega_p B_p}, \quad \frac{m_m}{\rho B_m^2} = \frac{m_p}{\rho B_p^2}, \quad \frac{I_m}{\rho B_m^4} = \frac{I_p}{\rho B_p^4} \text{ and } \zeta_m = \zeta_p \quad (17)$$

where ω denotes the torsional circular eigenfrequency or vertical bending circular eigenfrequency which will participate in flutter; U denotes mean wind speed; m and I denote the deck mass and inertial moment of mass per unit length, respectively. The mass and the inertial moment of mass of the main cables and those of the towers were transformed to the deck using a equivalent method given in (Xiang *et al.* 1996); B denotes the deck width; ρ denotes air density; ζ denotes the torsional or vertical bending damping ratio; subscripts m and p denote model and prototype, respectively. The sectional model was made at a scale of 1/60. The wind speed ratio was 1/9 for

Table 2 Critical flutter wind speeds (m/s)

Wind attack angle	Stage C			Stage D			Stage E		
	-3°	0°	+3°	-3°	0°	+3°	3°	0°	+3°
Sectional model	>150	>150	113	164	167	126	153	156	117
Aeroelastic model	>150	>150	135	>125	>125	125	>125	>125	118
Error (%)	/	/	16	/	/	0.8	/	/	0.8

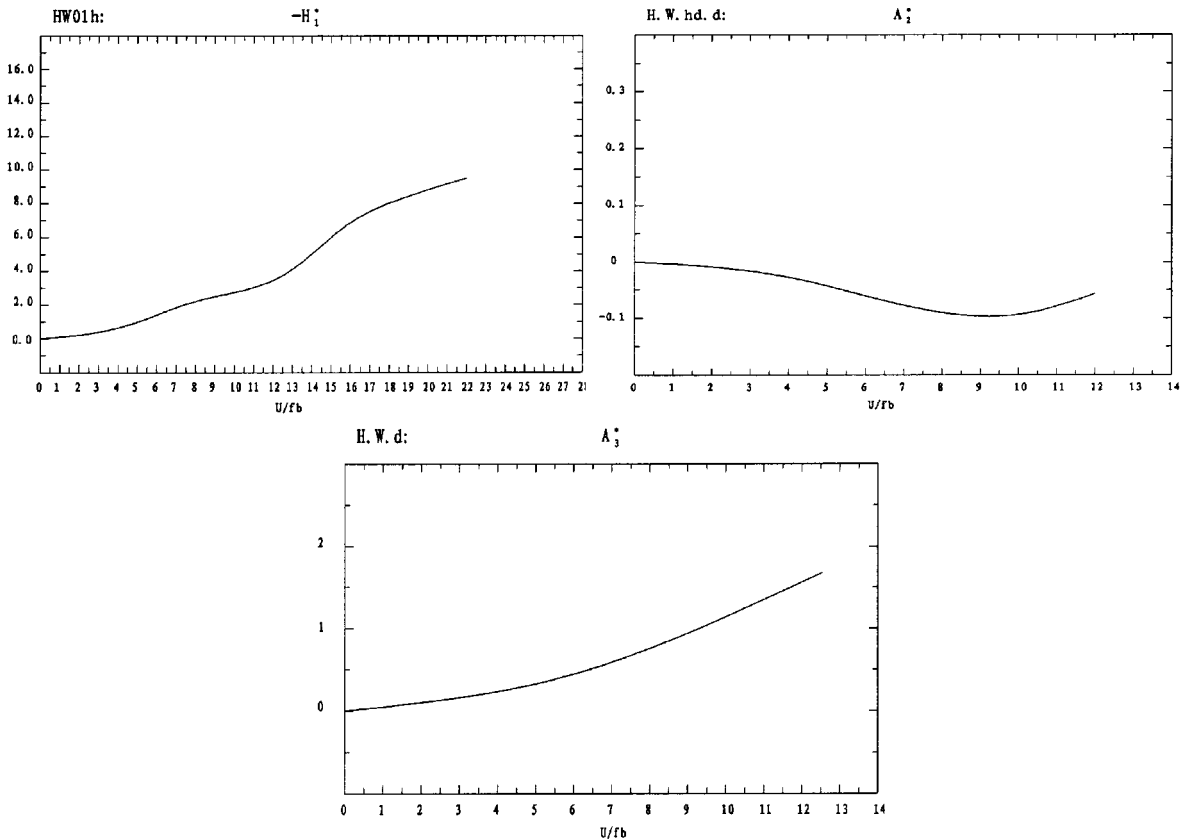


Fig. 6 Main flutter derivatives of the bridge deck for operation stage

both modes.

The critical flutter wind speeds of the bridge obtained from the sectional model test at the selected stages and the three wind attack angles are shown in Table 2, together with the corresponding results from the full bridge aeroelastic model test, which will be discussed later on. The critical flutter wind speeds at $+3^\circ$ wind attack angle at the three stages are all lowest compared with those at -3° and 0° wind attack angles. All the critical flutter wind speeds shown in Table 2 are higher than 100 m/s, so it is obvious that the aerodynamic stability of the Shantou Bay Bridge is quite well.

The flutter derivatives are then extracted from the acceleration signals from the test using CVR method (Xie 1987). The main flutter derivatives for the operation stage are shown in Fig. 6.

In addition, no obvious vortex-excited vibration was observed in the test. The largest response of the vortex-excited vibration of the bridge deck is about 1/9 smaller than the largest buffeting response.

6. Computation of buffeting response

Buffeting response is one of the most concerned problems in wind-resistant study of the Shantou Bay Bridge. The computation of the buffeting responses was performed and some main results are presented here.

In the analysis of the buffeting, the Kaimal's and Panofsky's expressions (Simiu and Scanlan 1978) of the wind speed spectra in longitudinal and vertical directions were adopted. The ground roughness length, z_0 , was determined to be 0.03 based on the terrain conditions around the bridge. The structural damping ratios for the analysis were assumed to be 0.02. The drag coefficients of the two main cables took 0.7, and the mean wind speed on the main cables took averagely 1 m/s higher than that on the bridge deck. The first three vertical mode buffeting responses were separately computed, and then the total vertical buffeting was composed of them using SRSS method; while only the first lateral buffeting and the first torsional buffeting were computed due to their much smaller values compared with the vertical one.

The aerodynamic admittances were postulated to be unity and Liepmann's simplified expression of Sears function, separately. The computations indicate that the buffeting responses are mainly contributed by the vertical bending modes for all the selected stages, more than 10 times larger than those contributed by the lateral or torsional modes, so only the vertical buffeting responses are presented here. The computed vertical buffeting responses with unity admittance and with the Liepmann's expression of Sear function are given in Fig. 7 together, in which the full lines denote the responses with Liepmann's expression of Sear function; the dotted lines denote those with unity admittances. In this figure the buffeting responses from the test of the full aeroelastic model of this bridge are shown as well, which are denoted with the symbol "o". From this figure, it is seen that the buffeting responses obtained from the test at the construction stages are closer to the computed results with the aerodynamic admittance of Sear function than to those with unity admittance; while the buffeting responses of the bridge at the operation stage are on the contrary. This seems to suggest that the vertical aerodynamic admittance of the Shantou Bay Bridge at the operation stage with parapets and anti-collision rails on the deck is close to unity; while the vertical aerodynamic admittance of the bridge deck without parapets, etc. on it, which is more streamlined than the deck at operation stage and closer to thin plate in configuration, may be replaced by the Sears function. From Fig. 7 it is seen that the maximum peak values (3.5 times RMS value) of vertical buffeting displacements at the operation stage, which appear at the quarter-span of the bridge, are about 0.6 m at 40 m/s deck level-wind speed, and about 1.3 m at 60 m/s deck level-wind speed. The maximum

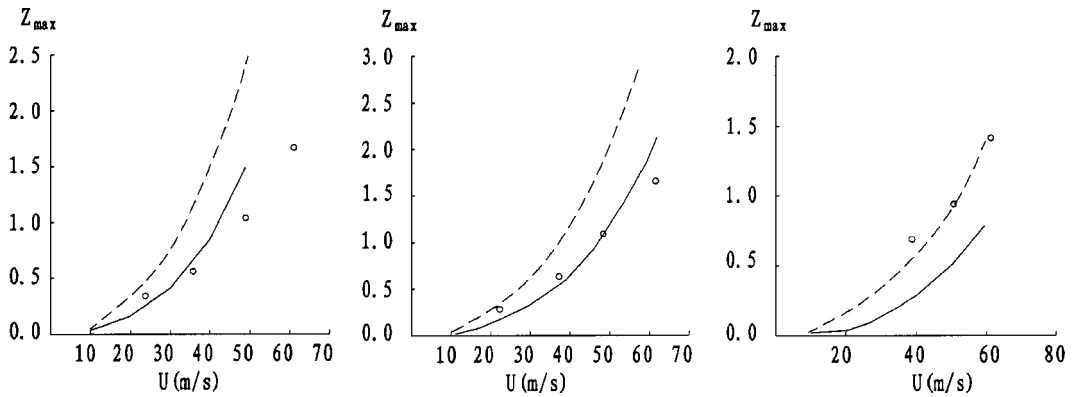


Fig. 7 Buffeting displacements of bridge at Stages C, D and E (Z_{max} in m)

peak buffeting displacements at the Stages D and C are about 0.6 m and 0.85 m at the buffeting design wind speed, namely 42 m/s, respectively.

7. Full bridge aeroelastic model test

In order to further check the aerodynamic stability and the buffeting response of the Shantou Bay Bridge, the full bridge aeroelastic model test was conducted.

7.1. Model design and fabrication

The wind tunnel for the full bridge aeroelastic model test has a working section of 5.15 m (W) \times 4.25 m (H). The dimensions of the wind tunnel and the total length of the bridge make the geometry scale of the model about 1/160. Further according to the diameter of high strength steel wire available from the market for the main cables of the bridge model, the model was finally made at a scale of 1/156. Thus the total length of the model is 4.87 meters. Fig. 8 shows the photo of the full



Fig. 8 Photo of the full bridge aeroelastic model in wind tunnel

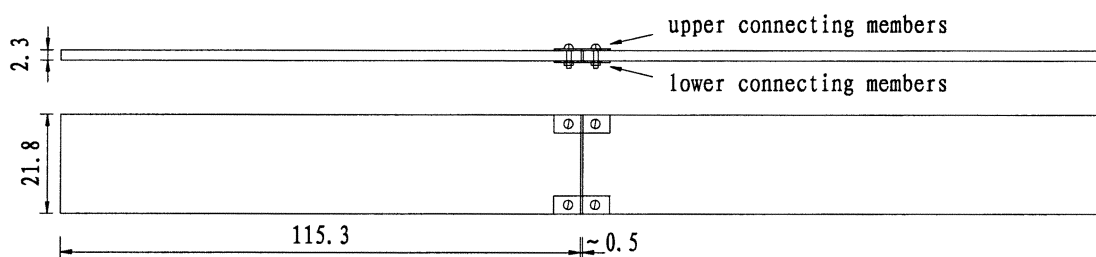


Fig. 9 Connection between sections of the aeroelastic model's deck

aeroelastic model in the wind tunnel. The test wind speed range is from 2 to 12 m/s. Re number of the full bridge aeroelastic model is about 1/3 of the sectional model.

The deck of the full aeroelastic model is composed of a core and a “clothing”. The former simulates the vertical bending stiffness, the lateral bending stiffness and the torsional stiffness; and the latter simulates the configuration of the deck. Additional mass blocks at appropriate positions simulate the required distributions of the mass and the inertial moment of mass of the bridge.

If a core has a rectangular cross section, it has only two design variables, i.e., the height and width of the cross section. Such a core, generally speaking, is difficult to meet the requirements of the simulation of these kinds of stiffnesses, that is, the vertical bending stiffness, the lateral bending stiffness and the torsional stiffness. In order that the deck core of the full aeroelastic model of the bridge had a most simple rectangular cross section, (E/G) was introduced as a new variable, simulating the ratio of the vertical bending stiffness and the torsional stiffness, where E and G are the modules of elasticity and the shear elasticity of the core material, respectively. Thus the deck core of the full bridge aeroelastic model could possess a rectangular cross-section, and the design of the model became much easier. H68 sheet brass with the value of 4.39 of (E/G) suits the requirement and was used in the design of the full aeroelastic model of the Shantou Bay Bridge.

Only one full aeroelastic model of the bridge was fabricated, simulating all the critical construction stages and the operation stage. For the prototype bridge, each deck section is temporarily connected to its neighboring sections during the construction stage. For the full bridge aeroelastic model, each deck section with a length of 115.4 millimeters, corresponding to three deck sections of the prototype bridge, was also connected to its neighboring sections with temporary connecting members. The core of the deck model and the temporary connecting members are shown in Fig. 9. In this figure, both the upper and lower connecting members are fixed on the core for simulating the operation stage; while only the lower connecting member is used for the construction stages. Determination of the sizes of the connecting members was based on experiments. Correspondingly, three hanging cables of the prototype bridge were merged into one hanging cable in the full bridge aeroelastic model.

The “clothing” of the deck of the model was made of plexiglass. Heating could easily curve the plexiglass to simulate the configuration of the bottom of the deck. The total mass and the inertial moment of mass per unit length of the deck model composed of the core and the “clothing” were both smaller than the corresponding design values, thus copper cubes were stuck to the deck of the model at appropriate positions to simulate the required distributions of the mass and the inertial moment of mass of the bridge.

7.2. Natural frequencies of the full bridge aeroelastic model

Natural frequencies of the full aeroelastic model are shown in Table 1, as mentioned before. It can be seen from Table 1 that the maximum error among the computed natural frequencies and the corresponding test values at the operation stage is 4%; and at the other stages the maximum error is about 7.8%. The frequencies presented in Table 1 indicate that the full aeroelastic model is satisfactory for simulation of the operation stage and the selected construction stages. The first vertical mode damping ratios for the Stages C, D and E were measured to be 1.78%, 1.74% and 1.1%, respectively; the first lateral damping ratios for the three stages 1.65%, 1.82% and 1.88%, respectively; and those for the first torsional modes 1.47%, 1.83% and 0.92%, respectively.

7.3. Critical flutter wind speed and buffeting response

Ten accelerometers, each of which has a weight of 0.5 grams, were used in the test to pick up the vibration acceleration signals of the full bridge aeroelastic model. Three accelerometers were mounted at the center of the main-span to measure the symmetric vertical, lateral and torsional mode vibrations, and other three accelerometers were mounted at the quarter-span to measure the asymmetric mode vibrations, and the others were placed on the tower and one side span.

The test for the critical flutter wind speeds was carried out in smooth flow; while the test for the buffeting responses was performed in turbulent flow. The simulation of the turbulent flow was achieved by a combination of a grid and a barrier at the entrance of the wind tunnel. The simulated turbulent intensity at the bridge deck level is about 10%; and the power spectrum at the same height and the central span is shown in Fig. 10. The longitudinal turbulent scale is about 36.5 cm. The wind attack angles in the tests were -3° , 0° and $+3^\circ$ which were achieved through bending and lifting the bracket on which the bridge model had been fixed. The test wind speeds from 2 to 12 m/s correspond to the real wind speed range of 25 m/s ~ 150 m/s, according to the wind speed ratio of 12.5.

7.3.1. Critical flutter wind speed

The full bridge aeroelastic model of the Shantou Bay Bridge was tested to obtain its critical flutter wind speeds at the Stages C, D and E. The results are given in Table 2, together with the sectional model test results for comparison. During the test, obvious divergent torsional vibrations of the

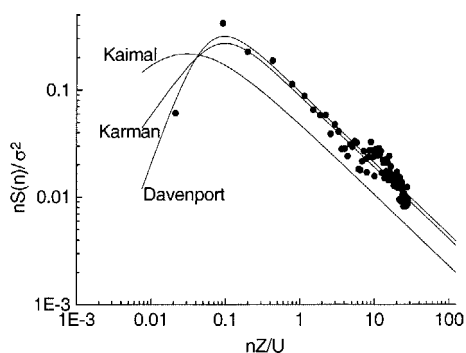


Fig. 10 Simulated power spectrum of fluctuating wind speed

model were observed when the wind speeds achieved the flutter critical values at $+3^\circ$ wind attack angles at all the three stages. The critical flutter wind speeds from the full aeroelastic model test presented in Table 2 further verify the aerodynamic stability of this bridge. It can also be seen that the critical wind speeds obtained from the full bridge aeroelastic model test are in good agreement with those from the sectional model test, especially for the Stages *D* and *E*. This seems to suggest, to a certain extent, that the effects of Reynolds number on the critical flutter wind speed of the Shantou Bay Bridge may be neglected.

7.3.2. Buffeting responses

The peak displacements of the bridge at the Stages *A*, *B* and *C* from the full bridge aeroelastic model test are presented in Fig. 7. The buffeting displacements from the test at the construction stages are seen to be closer to the computed displacements with Liepmann's expression-type vertical aerodynamic admittance function than to those with unity aerodynamic admittance function; but the buffeting displacements of the bridge at the operation stage are closer to the computed displacements with unity aerodynamic admittance. The comparison between the computed results and the test ones seems to indicate that the unity aerodynamic admittance function relatively suit the bridge at the operation stage; while aerodynamic admittance of the deck of the Shantou Bay Bridge at the erection stages may be approximately replaced by Sear function. This may be due to that the bridge deck at the erection stage without parapets and anti-collision rails on it is more stramlined than that at the operation stage.

In addition, the buffeting displacements from the full aeroelastic model test agree well with those from the computation. Reynolds number seems also to have no great effects on the buffeting responses of this bridge.

8. Conclusions

The critical flutter wind speeds of the Shantou Bay Bridge at the selected critical erection stages and the operation stage were obtained through the sectional deck model test. Then the buffeting responses of this bridge were analyzed using the Buffeting Response Spectrum method. Finally the full bridge aeroelastic model was tested to further check the flutter and buffeting characteristics. From the present researches some main conclusions are obtained as follows,

- (1) A method proposed in this paper could make the design and fabrication of a full bridge aeroelastic model much easier and more precise. In this method, (E/G) is introduced as a variable for simulating the ratio between the vertical bending stiffness and the torsional stiffness of the bridge deck. Thus a rectangular cross section can be chosen as the core of the deck of the full bridge aeroelastic model.
- (2) The critical flutter wind speeds of the Shantou Bay Bridge at the operation and the construction stages obtained from the full aeroelastic model test and from the sectional model test agree well with each other. The critical flutter wind speeds from these two kinds of model tests indicate that the aerodynamic stability of the Shantou Bay Bridge is satisfactory.
- (3) The buffeting responses are computed using Buffeting Response Spectrum method, and are obtained from the full bridge aeroelastic model test as well. For the Shantou Bay Bridge, the vertical aerodynamic admittance function at the erection stage may be approximated by Sears function; while those at the operation stage are close to unity.

Acknowledgements

This project is jointly supported by National Science Foundation for Outstanding Youth and Foundations for University Key Teacher by the Ministry of Education, which are gratefully acknowledged.

References

- Chen, X., Matsumoto, M. and Kareem, A. (1999), "Coupled flutter and buffeting response of bridges", *Proc. of 10th Int. Conf. on Wind Eng.*, Copenhagen, Denmark, 21-24 June, **2**, 845-850.
- Chen, W., Gu, M. and Xiang, H.F. (1995), "Study on buffeting response spectrum method for long-span bridges", *J. Wind Eng. Ind. Aerod.*, **54/55**, 83-89.
- Diana, G., Cheli, F., Zasso, A. and Boccilone, M. (1999), "Suspension bridge response to turbulent wind: Comparison of a new numerical simulation method results with full data", *Proc. of 10th Int. Conf. on Wind Eng.*, Copenhagen, Denmark, 21-24 June, **2**, 871-878.
- Gu, M. and Xiang, H.F. (1991), "Buffeting analysis of Nanpu cable-stayed bridge", *Proc. of the 3rd East Asia-Pacific Conf. on Struct. Eng. and Constr.*, Shanghai, China, April 23-26, **2**, 1543-1548.
- Jain, A., Jones, N.P. and Scanlan, R.H. (1996), "Coupled flutter and buffeting analysis of long-span bridges", *J. Struct. Eng.*, ASCE, **22**(7), 716-725.
- Liepmann, H.W. (1952), "On the application of statistical concepts to the buffeting problem", *J. Aeronaut. Sci.* **19**(12), 793-800.
- Scanlan, R.H. and Tomko, J.J. (1971), "Airfoil and bridge deck flutter derivatives", *J. Eng. Mech. Div.*, ASCE, **97**(EM6), 1717-1737.
- Scanlan, R.H. (1977), "Motion of suspended bridge spans under gusty wind", *J. Str. Div.*, ASCE, **103**(ST9), 1867-1883.
- Simiu, E. and Scanlan, R.H. (1978), *Wind Effects on Structures* (2nd Edition), John Wiley & Sons.
- Xiang, H.F. et al. (1996), *Chinese Guideline for Wind-resistance Design of Highway Bridges*, Renmim Jiaotong Publisher.
- Xie, J.M. (1987), "CVR method for identification of unsteady aerodynamic model", *Proc. 7th Int. Conf. on Wind Eng.*, Aachen, Germany, 273-281.